

Finite Element Comparison of 10 Orthodontic Microscrews with Different Cortical Bone Parameters

Jordi Marcé-Nogué, PhD¹/Andre Walter, MD, DDS, MS²/Lluís Gil, PhD³/Andreu Puigdollers, PhD⁴

Purpose: Unlike standard dental implants, the stabilization of orthodontic microscrews removed after treatment is done without osseointegration and achieved by several components: cortical bone thickness (CBT), microscrew geometry, and drilling depth. The purpose of this study was to evaluate 10 different microscrews and the influence of their geometric parameters with different CBT and drilling depths.

Materials and Methods: The influence of geometric parameters in cortical bone was analyzed with a series of computational simulations with finite element models to obtain von Mises stresses and deformations in the microscrew when loaded with a perpendicular traction force of 1 N and considering the angle of incidence as a random parameter. **Results:** There was variability in the angle of incidence, with less clinical influence. Biomechanical parameters such as microscrew diameter, CBT, and drilling depth had significant influences on the results. At a drilling distance of 8 mm, narrow microscrews (Abso Anchor 1.2) showed maximum von Mises stress of 500.698 MPa and maximum deformation in the shank of 0.08549 mm. Microscrews with a diameter of 1.5 mm (Dentaurum, Jeil, Mondeal, Tekka, Spider) showed von Mises stresses ranging from 56.97 to 136 MPa and deformation between 0.0062055 and 0.0476 mm. Microscrews with a diameter of 2.0 mm (Jeil, Mondeal, Tekka) showed von Mises stresses ranging from 17.172 to 54.861 MPa and deformation of 0.000172 to 0.0161 mm. **Conclusions:** The shape and geometry of an orthodontic microscrew are highly important in its behavior. Optimal characteristics of a microscrew would include a diameter of 2.0 mm, a cylindrical shape, a short and wide head, a short and wide shank, and threads of an appropriate size. INT J ORAL MAXILLOFAC IMPLANTS 2013;28:e177–e189. doi: 10.11607/jomi.2447

Key words: cortical bone, finite element method, microscrews, orthodontics, random, variance

Today, the use of oral implants and prostheses for treatment of partial and total edentulism has increased significantly as a viable alternative to removable dentures. The first implants used to anchor oral prostheses date back to the 1960s, when Per-Ingvar

Brånemark made his first in vivo experiments in canine bone structures and found that bone tissue could directly contact titanium surfaces without additional fibrous tissues at the interface. This discovery initiated the application of oral implants.

The use of titanium microscrews for orthodontics requires good stability and good resistance to failure. It is suggested that this stability is related to the quality and quantity of the cortical bone,¹ the geometric design of the microscrew,² and the amount of force applied at the site.³

It is important to determine the influence of the incidence angle of force applied as a consequence of traction in the teeth. This factor has not yet been considered; the results of other studies have been considered without any variation in the results if the traction force is applied at a different incidence angle. In the present study, variations caused by the location of the traction force will be considered because the shape of the thread in the location of force application will vary with the location of the force. This will be treated as a random variable and estimated as a normal distribution with standard deviations. This will allow comparison of different results obtained with variations in the incidence angle.

¹Researcher, Assistant Professor, Department of Resistance of Materials and Structures to Engineering, Escola Tècnica Superior d'Enginyeria Industrial i Aeronàutica de Terrassa, Universitat Politècnica de Catalunya, Terrassa, Spain.

²PhD Candidate, Associate Professor, Faculty of Dentistry, Universitat Internacional de Catalunya, Sant Cugat del Vallès, Spain.

³Lecturer, Department of Resistance of Materials and Structures to Engineering, Escola Tècnica Superior d'Enginyeria Industrial i Aeronàutica de Terrassa, Universitat Politècnica de Catalunya, Terrassa, Spain.

⁴Professor, Faculty of Dentistry, Universitat Internacional de Catalunya, Sant Cugat del Vallès, Spain.

Correspondence to: Dr Jordi Marcé-Nogué, Department of Resistance of Materials and Structures to Engineering, Escola Tècnica Superior d'Enginyeria Industrial i Aeronàutica de Terrassa, Universitat Politècnica de Catalunya, c/Colom 11, TR45 Building, 08222 Terrassa, Barcelona, Spain. Email: jordi.marce@upc.edu

©2013 by Quintessence Publishing Co Inc.

Table 1 Geometric Characteristics of Tested Microscrews

| | Microscrew | Screw length (mm) | Head diameter (mm) | Shank diameter (mm) | Shank length (mm) | Shank shape | Thread shape | Pitch (mm) |
|---|-------------------|-------------------|--------------------|---------------------|-------------------|-------------|--------------|------------|
| A | Abso Anchor 1.0 | 12.00 | 1.50 | 1.00 | 9.00 | Cylindric | Metric | 0.5 |
| B | Dentaurum 1.5 | 14.00 | 2.90 | 1.60 | 10.00 | Conical | Sawtooth | 1 |
| C | Jeil 1.6 | 12.00 | 3.15 | 1.60 | 9.00 | Cylindric | Sawtooth | 0.7 |
| D | Jeil 2.0 | 12.00 | 3.15 | 2.00 | 9.00 | Cylindric | Sawtooth | 0.7 |
| E | MAS Microbite 1.3 | 12.00 | 2.60 | 1.30 | 8.00 | Cylindric | Sawtooth | 0.6 |
| F | Mondeal 1.5 | 14.00 | 2.75 | 1.40 | 10.00 | Cylindric | Metric | 0.7 |
| G | Mondeal 2.0 | 14.50 | 2.75 | 2.00 | 10.00 | Cylindric | Metric | 0.7 |
| H | Spider Screw 1.5 | 13.50 | 3.00 | 1.35 | 9.00 | Conical | Sawtooth | 0.7 |
| I | Tekka 1.5 | 16.00 | 2.50 | 1.50 | 11.00 | Cylindric | Sawtooth | 0.625 |
| J | Tekka 2.0 | 15.25 | 2.50 | 2.00 | 11.00 | Cylindric | Sawtooth | 1 |

Another important issue with previous studies is that although several authors have examined variations in some important geometric parameters using finite element analysis (FEA)—for example, cortical bone thickness (CBT), diameter of the microscrew, and drilling depth—most of these studies assumed simplified geometries. The present study used the actual geometry of commercially available microscrews.

Therefore, the goal of this research is to compare the performance of different commercially available orthodontic microscrews using FEA from a new point of view. The incidence angle of the traction force will be considered in a statistical analysis because of its random variations, and the influence of geometric parameters such as CBT, the drilling depth of the microscrew into the bone, and the angle of application of the traction force will be studied.

The objectives of this study were to determine:

1. The influence of the diameter and length of microscrews on their stress and deformation at depths of 6, 7, and 8 mm in bone.
2. The influence of microscrew length on the stress and deformation of the screws.
3. The influence of primary stability on microscrew stress and deformation at 6 to 8 mm of depth within bone.
4. The influence of unfavorable conditions (thin cortical bone, shallow drilling depth) on microscrew stress and deformation at a depth of 6 mm within bone.
5. The influence of the shape of the microscrews (cylindric vs conical) on stress and deformation.

MATERIALS AND METHODS

A series of computational simulations were performed using the finite element software ANSYS 12.0 to evaluate the stress state and deformation of the microscrews when they were loaded perpendicularly with a traction force of 1 N. A microscrew is a small bone screw, usually made of titanium or titanium alloy, between 1.2 and 2.2 mm in diameter and 5 to 15 mm in length. These screws are placed transmucosally, and an attachment mechanism is left exposed in the oral cavity to relocate teeth. The traction force is the approximate orthodontic force applied to a microscrew in clinical practice by the attachment mechanism when teeth are moving (and by a plate in the present model).

Models

The commercially available microscrews studied were manufactured by Abso Anchor, MAS Microbite, Spider Screw, Tekka, Mondeal, Jeil, and Dentaurum; their characteristics are listed in Table 1. The computer models were built beginning with pictures taken in a digital microscope of the original microscrews, with the models carefully created from the dimensions measured digitally (Fig 1).

The 10 models were absolutely different in geometric parameters, such as the diameter of the shank, the shape of the thread, the length of the shank, and particularly the shape of each screw. The behavior of each commercial microscrew and the comparisons between them will be studied according their particular geometry and the geometric parameters of the cortical bone.

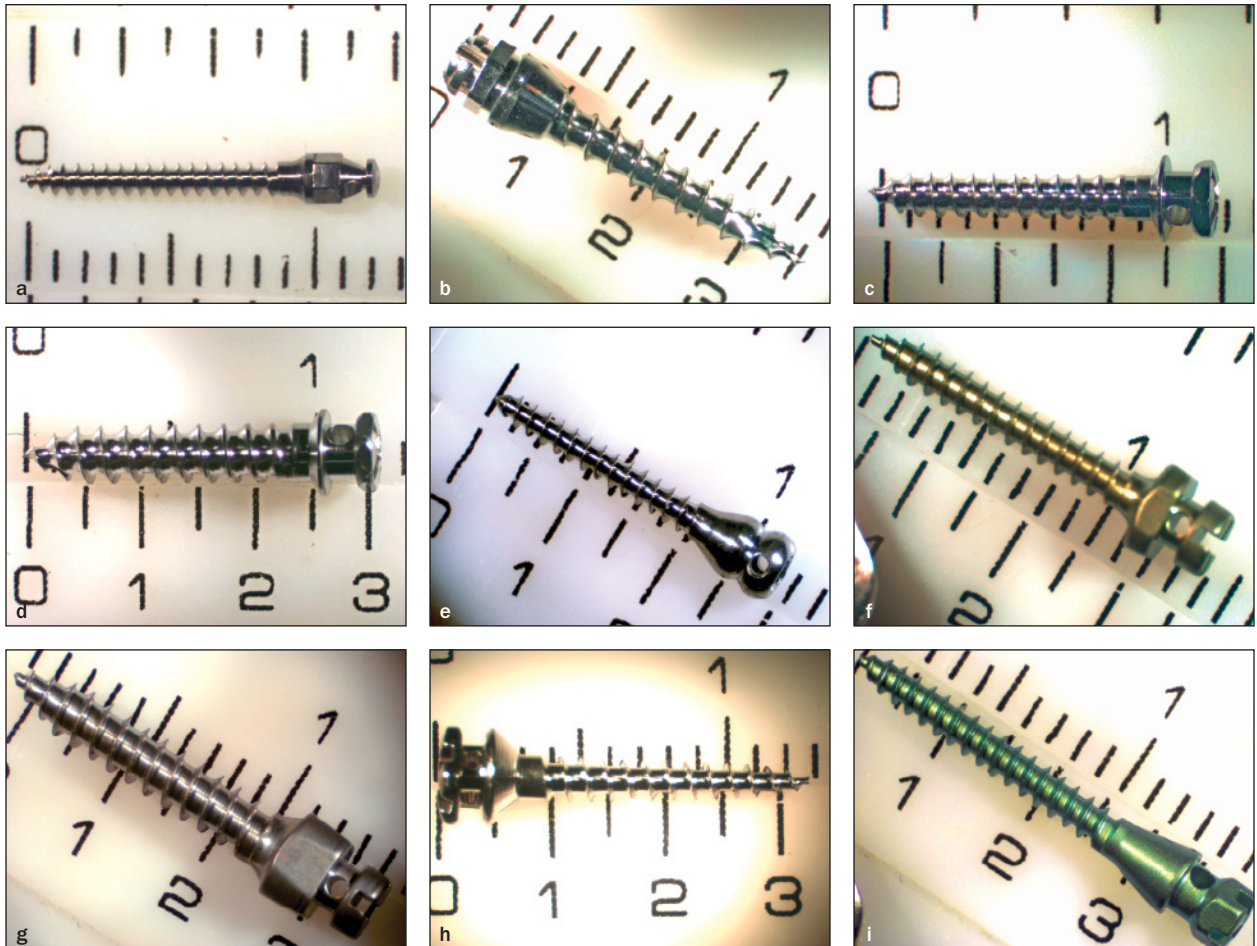
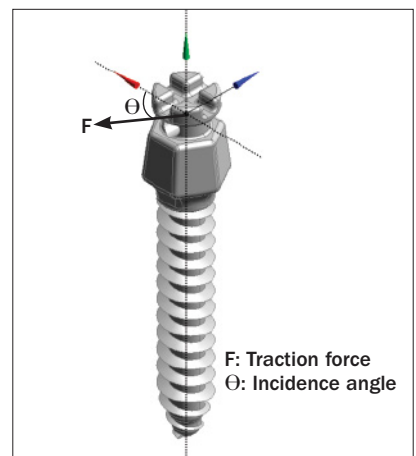


Fig 1 The microscrews tested, all of which are used in clinical practice (see Table 1).



Fig 2 (right) Incidence angle of the traction force in the model.



F: Traction force
 Θ: Incidence angle

Analyses

Analysis of the Incidence Angle. The main purpose of this first study was to evaluate a wide range of values of the incidence angle (Fig 2), between 0 and 360 degrees, to determine its influence in the analysis of cortical bone parameters. The incidence angle is the angle between the force applied by the plate and an arbitrarily chosen (but always the same) point on the shank. Because the threads will generate different geometries in the shank when the position of the incidence angle varies, this change of geometry was taken into account in the data recorded.

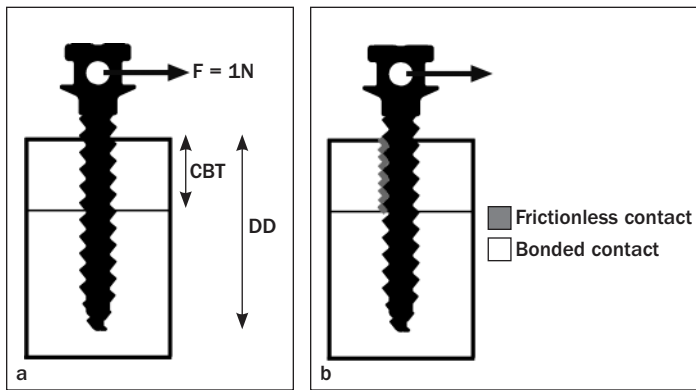


Fig 3 (a) Geometric parameters studied in the cortical bone; (b) contacts applied in the FE model.

However, the twist of the micro-screw is a random variable because, first, the final position of the screw when it is situated in the bone is not known, and second, its position depends on different random variables such as the force applied by the dentist, the initial position of the threads when insertion begins, etc. The final position of the micro-screw in the maxillofacial bone is therefore unknown and can be considered random. For this reason, and considering the different data obtained by variations in the incidence angle, a statistical analysis was planned for each different position of the force (Fig 2). Normal distributions with standard deviations were obtained for each micro-screw.

Analysis of Cortical Bone Geometric Parameters.

Some parameters of the bone were modified to study the combined influence of these parameters: drilling depth of the micro-screw into the bone (DD) and CBT (Fig 3a). DD was set at 7 or 8 mm, and CBT was set at 1, 2, or 3 mm. The results were analyzed in terms of these parameters and their influence.

Material Properties

The maxillofacial bone was defined by its two typical types: cancellous bone, which typically occupies the interior region of bones, is highly vascular, and frequently contains red bone marrow; and cortical bone, which, as its name implies, forms the cortex, or outer shell, of most bones. It is much denser, harder, stronger, and stiffer than cancellous bone. Table 2 details the elasticity and Poisson ratios taken from the literature and used for the various parts of the model.

Interface Surfaces

Two bodies are in contact when two separate surfaces of each body touch each other in such a way that they become mutually tangential. The contact surface between the titanium micro-screw and the bone was modeled using a bonded contact in the cancellous bone and a frictionless contact in the cortical bone (Fig 3b).

Table 2 Properties of the Modeled Materials

| Material | Modulus of elasticity (MPa) | Poisson ratio |
|-------------------|-----------------------------|---------------|
| Cortical bone | 17,000 | 0.3 |
| Cancellous bone | 90 | 0.3 |
| Surgical titanium | 110,000 | 0.35 |

The cancellous bone was considered to be osseointegrated (bonded) with the micro-screw. The bonded contact assumes no gaps between the bodies and it is suitable for this behavior. Its formulation is a penalty-based contact formulation with high normal stiffness by default (Equation 1).

$$(1) \quad F_{normal} = k_{normal} X_{penetration}$$

The frictionless contact for cortical bone assumes that a gap is allowed during normal behavior and sliding is allowed during tangential behavior. An augmented Lagrange formulation (Equation 2) and auto-asymmetric behavior were assumed, in which only the contact surfaces were constrained from penetrating the target surfaces. The default normal stiffness *k* was determined automatically by the FEA package.

$$(2) \quad F_{normal} = k_{normal} X_{penetration} + \lambda$$

This implies a nonlinear solution and, for instance, a convergence iterative procedure, which was automatically activated by the software by means of a Newton-Raphson iterative algorithm.

Convergence of the Mesh

A mesh of hexahedric and tetrahedric elements was created for each model (Fig 4). An initial refined mesh was automatically generated by the FEA software, and convergence tools were used as part of the solution process (h-adaptive method). This was done by the FEA software, which controlled the level of accuracy for selected results of stress and employed an adaptive solver engine to identify and refine the model in areas that would benefit from adaptive refinement. In this case, the mesh of the shank was of greatest interest, since the authors wished to evaluate its stress state.

The Zienkiewicz-Zhu norm^{4,5} for stress in structural analysis was used to control the element’s results and

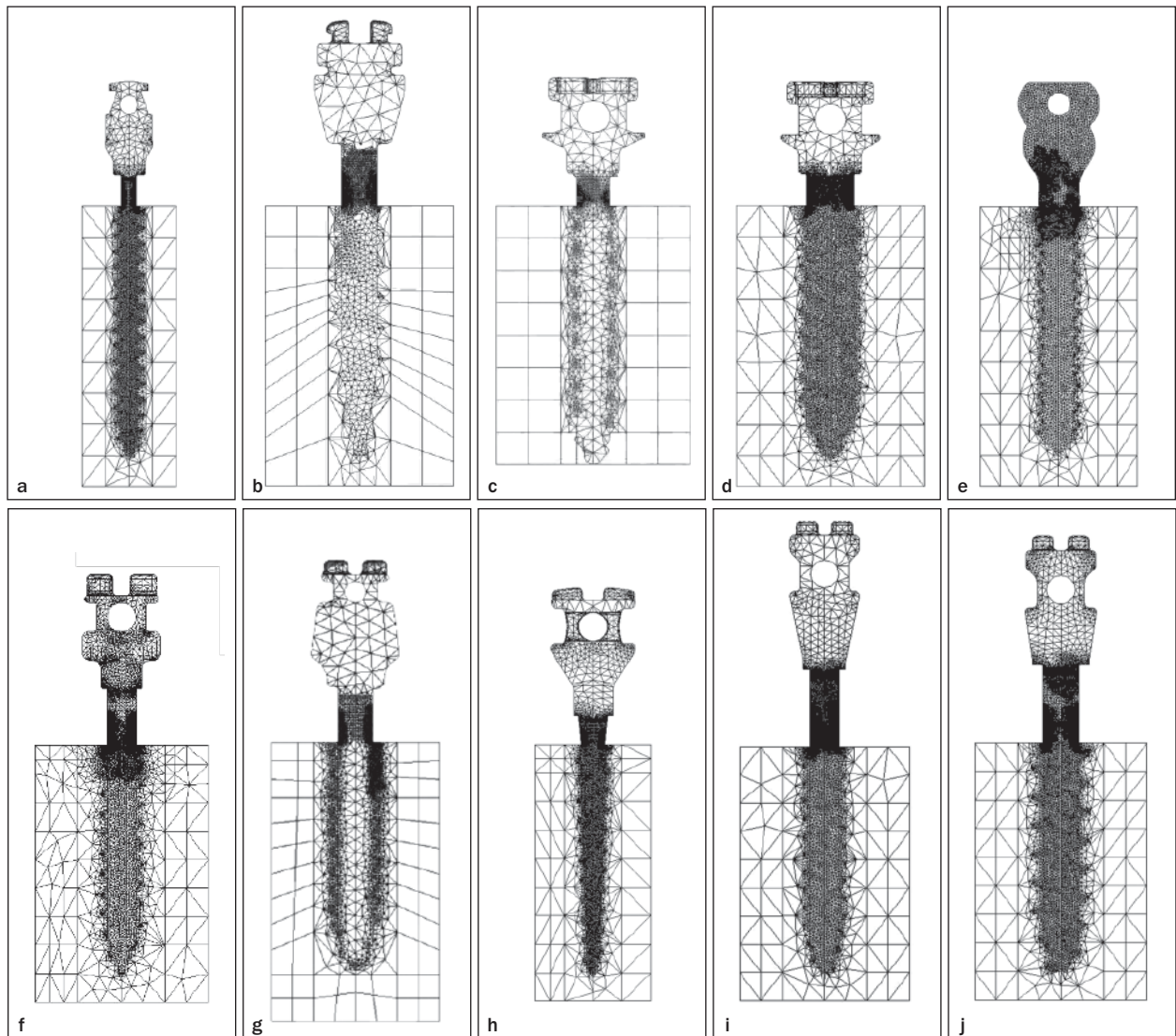


Fig 4 Converged resulting meshes of microscrews A through J (see Table 1).

the convergence when possible. When the convergence of the energy error in a particular element was not satisfied (Equation 3), a new refined mesh was created for this element to evaluate the new stress values.

$$(3) \quad \left(\frac{\sigma_{i+1} - \sigma_i}{\sigma_i} \right) < \left(\frac{e}{U + e} \right)^{\frac{1}{2}}$$

In this equation, i denotes the iteration number, σ is the von Mises stress, e is the energy error, and U is the strain energy. These results were compared from iteration i to iteration $i + 1$. Iteration in this context included a full analysis in which h-adaptive meshing and solving were performed.

The energy error was obtained from the evaluation of the stress values in the nodes of the N elements of the domain (Equation 4), where D is the stress-strain matrix and $\Delta\sigma$ the stress error vector. In $\Delta\sigma$ (Equation 5), where the value of the stress vector of node n of element i is obtained, the stress vector σ and the averaged stress vector at node n are considered in relation to the number of elements N_e connecting to node n .

$$(4) \quad e = \sum_{i=1}^N \frac{1}{2} \int_V \Delta\sigma^T D^{-1} \Delta\sigma dV$$

$$(5) \quad \Delta\sigma_n^1 = \frac{\sum_{i=1}^{N_e} \sigma_n^i}{N_e} - \sigma_n^i$$

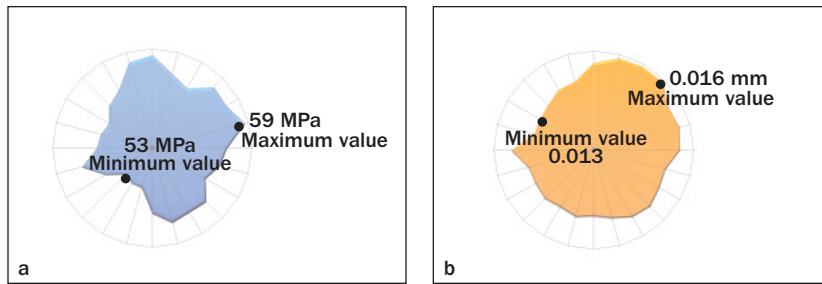


Fig 5 Variations of the (a) maximum von Mises stress in the shank and (b) maximum total displacement in the screw, as influenced by the incidence angle, for model B.

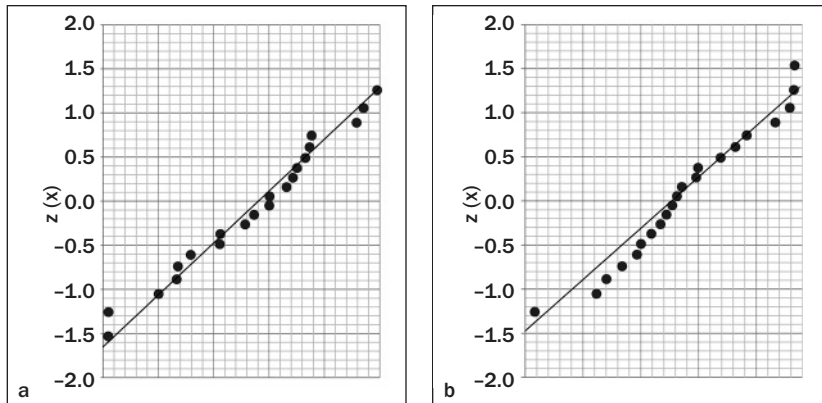


Fig 6 Cumulative distribution function for (a) maximum stress in the shank and (b) maximum deformation of model B.

Table 3 Variations in the von Mises Stress and Deformation

| Microscrew | Stress variance (MPa) | Deformation variance (mm) |
|---------------------|-----------------------|---------------------------|
| A Abso Anchor 1.0 | 4.179 | 0.00092 |
| B Dentaurum 1.5 | 0.96 | 0.00010 |
| C Jeil 1.6 | 0.902 | 0.000057 |
| D Jeil 2.0 | 0.24 | 0.00001 |
| E MAS Microbite 1.3 | 1.74 | 0.00015 |
| F Mondeal 1.5 | 0.92 | 0.00022 |
| G Mondeal 2.0 | 0.48 | 0.0001 |
| H Spider Screw 1.5 | 0.51 | 0.00017 |
| I Tekka 1.5 | 1.64 | 0.000262 |
| J Tekka 2.0 | 1.16 | 0.000126 |

RESULTS

Influence of the Incidence Angle

Variations in the incidence angle in the screw will generate different amounts of displacement in the head of the screw and different stress values in the shank. Figure 5 shows, along the entire range of values of the incidence angle, variations in the maximum von Mises stress values in the shank and the maximum displacement values of the screw in one of the models considered in the whole range of incidence angles. The maximum and minimum values are also shown.

These results show that there is certain variability related to the position of the traction force. The cumulative distribution function of each data set was obtained and, because they were reasonably aligned, the normal distribution was confirmed (as can be observed in Fig 6 for microscrew B). Consequently, the variance of each model could be obtained (Table 3, Fig 7) and analyzed in the following results, depending on whether the incidence angle was considered a random variable.

Stress, Deformation, and the Influence of CBT

Results were recorded for each of the 10 models to quantitatively compare the behavior of the models considered. The maximum values for von Mises stresses and deformation in the shank are shown in Table 4 (DD 8 mm) and Table 5 (DD 6 mm).

The displacement (deformation) of the microscrew was obtained at three specific points: A = the top of the head of the microscrew, where the displacement is maximal; B = at the point where the force was applied; and C = at the place where the screw entered the bone (Fig 7). Points A and C coincide in each model, but point B differed depending on the model and the manner in which the model allowed the force to be sited. The main interest in point B was to compare the displacement of the point at which the load was applied, and it will be considered a target of optimization in its minimum values (Fig 8a shows the total deformation of the microscrew).

Stresses should be observed in a place without artificial noise in which the convergence criterion of the mesh can be applied. A good place is the part of the

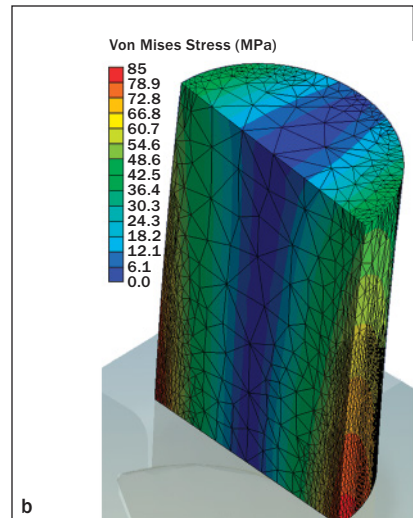
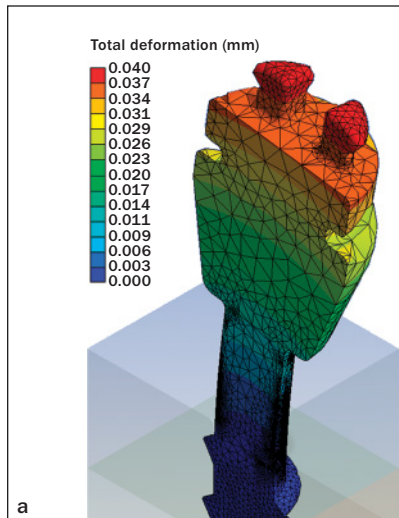
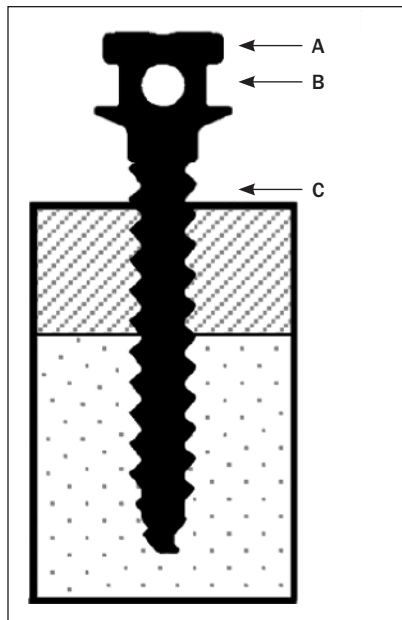


Fig 7 (Left) Specific points on the screw that were used to determine the amount of displacement.

Fig 8 (Above) Model B. (a) Total deformation; (b) von Mises stress in the shank.

shank outside the bone, where the threads are not engaged in bone. The threads can be omitted from the analysis and, consequently, the artificial noise in the complex geometry of the helical threads is avoided. Moreover, the convergence criterion of the mesh can be applied, and this procedure guarantees the correctness of the stress values obtained (Fig 8b shows the von Mises stresses at this part of the shank).

The von Mises criterion is an isotropic criterion that is traditionally used to predict the yield point of ductile materials such as metals. It assumes equal strength in tension and compression, which is not very realistic in bone tissue because bone is a fragile material and a fragile criterion should be used. Nevertheless, according to Doblaré et al,⁶ when isotropic material properties are used in cortical bone, the von Mises criterion may be the most accurate for predicting fracture location, even after accounting for differences in the tensile and compressive strength of bone.

Stress results in the shank, shown in Table 4 for a DD of 8 mm, shows that there was a strong influence of screw diameter, and CBT was less influential. A wide range of results was seen, especially when comparing Abso Anchor 1.0 (500.698 MPa) with Jeil 2.0 (17.172 MPa). Several microscrews with a diameter between 1.5 and 1.6 mm showed similar results—ie, Dentaurum 1.5 (57.97 MPa), Jeil 1.6 (56.137 MPa), and Mondeal 1.5 (88.474 MPa)—but stresses were much higher for Tekka 1.5 (121.045 MPa) and Spider 1.5 (136 MPa). When the DD was 6 mm (Table 5), the results were, as expected, worse for all microscrews but especially for the narrowest:

Abso Anchor 1.0 (500.698 to 825.50 MPa) and MAS Microbite 1.3 (27.748 to 105.287 MPa).

The stress values for microscrews of intermediate size showed mixed results, ranging from 83.078 MPa (Dentaurum 1.5) to 224.795 MPa (Spider 1.5). Two microscrews that were 2 mm in diameter (Tekka 2.0 and Mondeal 2.0) displayed similar results (78.95 and 74.156 MPa), whereas the Jeil 2.0 had a lower value (28.16 MPa).

Table 4 shows the maximum deformation at a DD of 8 mm. The best results were obtained for Jeil 2.0 (0.0017204 mm), MAS Microbite 1.3 (0.0044386 mm), and Jeil 1.6 (0.0062055 mm); intermediate results were seen for Mondeal 2.0 (0.012 mm), Dentaurum 1.5 (0.015 mm), and Tekka 2.0 (0.016 mm); and the worst results were seen with Mondeal 1.5 (0.022 mm), Spider 1.5 (0.0224 mm), Tekka 1.5 (0.047 mm), and Abso Anchor 1.2 (0.085 mm). At a DD of 6 mm (Table 5), deformation was greater, and variations in CBT affected Tekka 1.5 (0.104 to 0.113 mm), Mondeal 1.5 (0.058 to 0.064 mm), and Abso Anchor (0.377 to 0.382 mm) more strongly than the other microscrews.

DISCUSSION

General Overview

Implant performance is usually assessed with experimental tests. The mechanisms leading to implant failure remain unknown because these data are difficult to obtain experimentally, but these factors can be studied

Table 4 Maximum von Mises Stress and Deformation in the Shank with a Drilling Distance of 8 mm and CBT of 3, 2, or 1 mm

| Microscrew | Maximum von Mises Stress (MPa) | | | Maximum deformation in the shank (mm) | | |
|---------------------|--------------------------------|---------|---------|---------------------------------------|-----------|-----------|
| | 3 mm | 2 mm | 1 mm | 3 mm | 2 mm | 1 mm |
| A Abso Anchor 1.0 | 500.698 | 500.186 | 501.955 | 0.08549 | 0.0854888 | 0.087493 |
| B Dentaurum 1.5 | 57.97 | 58.05 | 58.711 | 0.015382 | 0.015895 | 0.020753 |
| C Jeil 1.6 | 56.137 | 55.164 | 55.022 | 0.0062055 | 0.006308 | 0.007609 |
| D Jeil 2.0 | 17.172 | 17.172 | 17.454 | 0.0017204 | 0.0018258 | 0.0027824 |
| E MAS Microbite 1.3 | 27.748 | 27.729 | 27.763 | 0.0044386 | 0.00452 | 0.005755 |
| F Mondeal 1.5 | 88.474 | 88.649 | 88.197 | 0.02203 | 0.02244 | 0.02542 |
| G Mondeal 2.0 | 54.861 | 54.785 | 53.371 | 0.012499 | 0.0127 | 0.01562 |
| H Spider Screw 1.5 | 136.00 | 135.592 | 135.43 | 0.0224549 | 0.02254 | 0.02459 |
| I Tekka 1.5 | 121.045 | 120.737 | 126.712 | 0.0476136 | 0.04792 | 0.05295 |
| J Tekka 2.0 | 54.751 | 55.558 | 56.399 | 0.0161 | 0.01633 | 0.0199 |

Table 5 Maximum von Mises Stress and Deformation in the Shank at a Drilling Distance of 6 mm and CBT of 3, 2, or 1 mm

| Microscrew | Maximum von Mises Stress (MPa) | | | Maximum deformation (mm) | | |
|---------------------|--------------------------------|---------|---------|--------------------------|------------|-----------|
| | 3 mm | 2 mm | 1 mm | 3 mm | 2 mm | 1 mm |
| A Abso Anchor 1.0 | 825.5088 | 823.86 | 825.18 | 0.37766 | 0.379457 | 0.3821349 |
| B Dentaurum 1.5 | 83.078 | 83.083 | 83.875 | 0.032042 | 0.03243 | 0.03771 |
| C Jeil 1.6 | 96.602 | 96.521 | 96.302 | 0.02461 | 0.024839 | 0.02802 |
| D Jeil 2.0 | 28.16 | 28.1819 | 27.474 | 0.005833 | 0.00606113 | 0.00834 |
| E MAS Microbite 1.3 | 105.287 | 105.792 | 104.7 | 0.02661 | 0.02679 | 0.03 |
| F Mondeal 1.5 | 128.02 | 127.77 | 127.13 | 0.05817 | 0.05844 | 0.06473 |
| G Mondeal 2.0 | 74.156 | 74.186 | 75.948 | 0.030658 | 0.031094 | 0.036211 |
| H Spider Screw 1.5 | 224.795 | 225.23 | 225.137 | 0.08026 | 0.0804 | 0.08404 |
| I Tekka 1.5 | 162.42 | 162.237 | 161.229 | 0.10452 | 0.105 | 0.11386 |
| J Tekka 2.0 | 78.95 | 78.88 | 81.218 | 0.03597 | 0.03647 | 0.04245 |

using computational methods. It is in this field that several quantitative studies of CBT have been performed to study the success rate of orthodontic mini-implants. For example, Motoyoshi et al¹ observed a relationship between success rate and CBT; they concluded that implants placed in an area with CBT > 1.0 mm had a better success rate and situated the clinical threshold for successful implantation in mini-implants at a diameter between 1.5 and 2.0 mm. Wilmes et al⁷ also analyzed the factors that influenced the primary stability of mini-implants and concluded that implant design, including diameter and length, had a great impact on the primary stability of mini-implants for orthodontic anchorage.

It has been previously demonstrated that design is an important parameter in stability.^{8,9} Moreover, all studies have considered the stress analysis and the maximum von Mises stress placed on the threads as

the main means of comparing the geometric variations of mini-implants.⁸⁻¹⁰ Some authors¹¹ have studied the influence of thread pitch on the von Mises values or the effect of using a washer.¹² These studies are more accurate, but they were done with dental implants and not with actual orthodontic microscrews.

Apparently, and considering only the results obtained in the present computational simulations, the behavior of the different models of commercial microscrews was qualitatively similar. Application of force resulted in bending of the microscrews, with the greatest lateral displacements seen in the head and the highest stresses seen in the shank as a cantilever beam. In general, for each microscrew, the displacements were greater when CBT was lower, and the stresses were higher when the DD was shallower. However, it is the numeric comparison and the statistical analysis that will provide the main

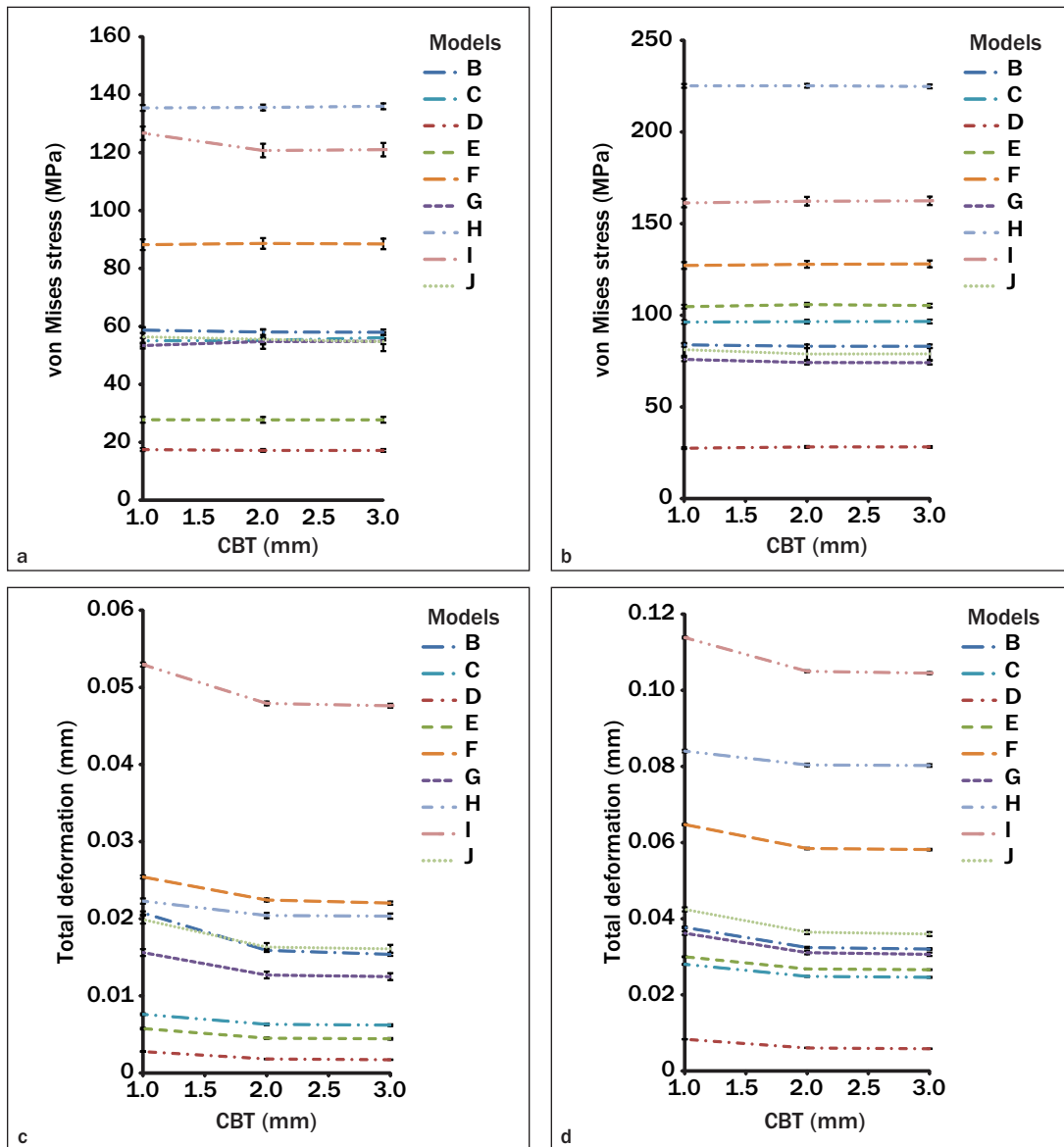


Fig 9 Maximum von Mises stress on (a) the shank for DD of 8 mm; maximum von Mises stress on (b) the shank for DD of 6 mm; total deformation of (c) the microscrews for DD of 8 mm at point A; total deformation of (d) the microscrews for DD of 6 mm at point A. Stresses for model A are not shown because of their high values.

quantitative information on the behavioral differences between the microscrews and will allow comparison of the different commercial models.

DD and CBT contributed significantly to the behavior of the microscrews. For favorable situations (sufficient DD and thick cortical bone), the behavior of most screws was quite similar in stress and deformation, but in unfavorable situations (short DD and thin cortical bone) some of the microscrews performed better than others. The deformations were higher in the screw heads and the stresses were higher in the shank with shorter DD, but CBT appeared to have no influence on the stress behavior of the shank.

The different data obtained for each microscrew are compared in Figs 9a to 9d. In each figure, the previously calculated variances were considered for its corresponding parameter, where two standard deviations from the mean account for about 95% of the set ($\hat{\mu} \pm 2\sigma^2$). For the von Mises stress results, model A stresses were not included because of their higher values (Tables 4 and 5). Quantitatively speaking, the behavior of this microscrew was absolutely different from that of the others in terms of both stresses and deformations. This was particularly true for stresses, where the values were much higher than the values of other microscrews; for this reason, model A cannot

be considered in this comparison. The fact that Abso Anchor 1.0 showed the highest stresses makes geometric sense, as it was the narrowest screw tested (diameter 1.2 mm).

Influence of DD

With respect to the stress values obtained in each microcrew (Table 4), when the DD was 8 mm, regardless of CBT, Abso Anchor 1.0 showed the worst behavior. Stresses were approximately eight or nine times higher than for the 1.5-mm-diameter microscrews, and for this reason (as mentioned earlier), it was not included in the figures.

Figure 9b shows how an unfavorable situation (DD of 6 mm) changed the behavior of the microscrews: the difference between Spider Screw 1.5 and Tekka 1.5 increased substantially, and Dentaurum 1.5 and Jeil 2.0 improved versus the other models. Tekka 2.0 displayed a similar behavior with respect to microscrews with diameters of 1.5 or 1.6 mm.

Figures 9c and 9d show that the deformation of some of the microscrews changed substantially when the DD changed. The screw with the greatest deformation was the conical-shaped Spider Screw 1.5, followed by Mondeal 1.5, Mondeal 2.0, Tekka 1.5, and Tekka 2.0. In contrast, Jeil 1.6 and Jeil 2.0 showed the least deformation. Dentaurum 1.5 displayed an intermediate behavior.

According to Table 4, in the group of microscrews with a diameter of 1.5 mm (Dentaurum 1.5, Mondeal 1.5, Spider Screw 1.5, and Tekka 1.5) there was a wide range of values, probably a result of the different shapes and sizes of each model. Although Dentaurum 1.5 and Mondeal 1.5, which have the same screw length, displayed similar behavior, Dentaurum 1.5 has a conical shape in the shank, while Mondeal 1.5 has a cylindrical shank. Looking at the results of the conical shape, despite being shorter, Spider Screw 1.5 displayed a stress state that was two times worse than that seen for Dentaurum 1.5. The taper of Spider 1.5 (high taper and small threads) was much higher than the taper of Dentaurum 1.5 (very low taper and big threads), and that appears to have influenced the results.

The influence of screw length can be observed in the stress values for Tekka 1.5 and Tekka 2.0, which are longer than the other microscrews; consequently the stresses were higher (two times that of Dentaurum 1.5). Finally, the microscrews with a diameter of 2.0 mm (Jeil 2.0, Mondeal 2.0, Tekka 2.0) showed similar values for maximum von Mises stress, but Jeil 2.0 displayed lower values because it was the shortest of these screws.

Considering the deformation values obtained in each microcrew, at a DD of 8 mm, deformations were lower than with a DD of 6 mm. In the case of an 8-mm DD with CBT of 3 mm, the microscrews with a diameter of 2.0 mm had, as expected, the best behavior (Table 4).

Mondeal 2.0 and Tekka 2.0 displayed similar results, while Jeil 2.0 had deformation that was five times less. Jeil 2.0 displayed the least deformation. With respect to the microscrews with a diameter around 1.5 mm, the values were fairly similar, except for the deformation obtained for Jeil 1.6. Despite the mere 0.1 mm of additional diameter, the maximum deformation value was much lower than that of the others (Dentaurum 1.5, Mondeal 1.5, Spider Screw 1.5, and Tekka 1.5). This difference cannot be attributed only to the difference in diameters.

With respect to the stress values measured at each microcrew (Table 5), when the DD was 6 mm, the narrower microscrews endured higher stresses in their shank (Abso Anchor 1.0 and MAS Microbite 1.3). In the case of a CBT of 2 mm, the microscrews with about 1.5 mm of diameter (Dentaurum 1.5, Jeil 1.6, Mondeal 1.5, Spider Screw 1.5, and Tekka 1.5) displayed an increase of approximately 40% in stress with a DD of 8 mm (except for the conical Spider Screw 1.5, for which the value was 75%) higher. The microscrews with a diameter of 2 mm showed stress increases of about 30%.

With respect to deformation (Table 5), when the DD was 6 mm, the least amount of deformation was seen for Jeil 1.6, Jeil 2.0, Mondeal 2.0, and Tekka 2.0. In the case of Jeil 2.0, the deformation was four times lower than for the other models with the same diameter (Mondeal 2.0 and Tekka 2.0). On the other hand, the narrower models (Abso Anchor 1.0 and MAS Microbite 1.3) and Spider Screw 1.5 showed more deformation. In spite of its conical shape, Dentaurum 1.5 showed similar values to the models with a diameter of 2.0 mm (Mondeal 2.0 and Tekka 2.0). This may be a result of the pitch of the threads, which was substantially greater than most of the others.

Summarizing the information shown in Fig 9, the change of the DD from 8 to 6 mm resulted in an increase in deformation by 50% to 70% in most of the microscrews. For the narrower screws (Abso Anchor 1.0 and MAS Microbite 1.3), this increase was even greater, reaching 80%.

Influence of CBT

Figures 9a and 9b show that differences in CBT were not important in the von Mises stress values of the microscrews. All of them displayed similar behavior upon variations in CBT (ie, the slope of the graph is practically zero) despite the differences in their geometric parameters.

With respect to deformation, it was greater with a CBT of 1 mm than when the CBT was 2 or 3 mm. This behavior in relation to the CBT was as expected by some authors,¹ who set the clinical threshold for the success of mini-implants at a diameter between 1.5 and 2.0 mm.

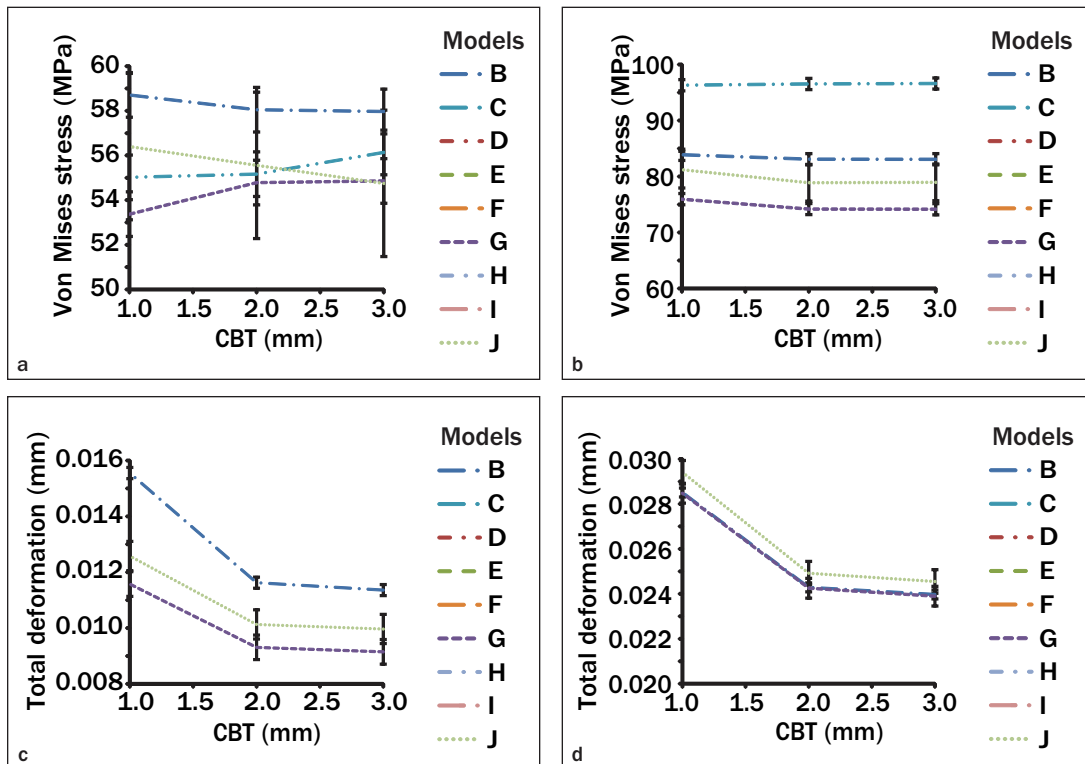


Fig 10 Maximum von Mises stress on (a) the shank for DD of 8 mm in models B, C, G, and J; maximum von Mises stress on (b) the shank for DD of 6 mm for models B, C, G, and J; total deformation of (c) the microscrews for DD of 8 mm at point B for models B, G, and J; total deformation of (d) the microscrews for DD of 6 mm at point B for models B, G, and J.

Influence of Variances in Incidence Angle

Figures 10a and 10b show the variance of the von Mises stresses caused by the random position of the incidence angle of the load for some of the microscrews (Dentaurum 1.5, Jeil 1.6, Mondeal 2.0 and Tekka 1.5). The variance is shown in each point of the graph with a black bracket indicating the threshold of values from the mean. The stress state in the shank when the DD is 8 mm for some models must be considered exactly the same because the variances showed relationships between the possible values. For a shorter DD, the recorded values of the stress state in the shank of the same microscrews must be considered different, because each variance is not linked to the others, and all the possible values considering this random variable will be different for each model. This means that, in favorable situations, these microscrews have the same stress state in the shank.

Figures 10c and 10d show the maximum deformation of the shank and variances of the incidence angle. There is no relationship between the values of each range, and this means that the maximum deformation of each microscrew can be considered different. In the same way, the values for deformation at point B, where

the traction force is applied, were compared. Taking into account the variance range, the behavior of most of the microscrews can be considered different. However, for a sufficient DD, two microscrews (Tekka 2.0 and Mondeal 2.0) can be considered to display the same behavior and, for a short DD, the microscrews Dentaurum 1.5, Mondeal 2.0, and Tekka 2.0 can be considered to display the same deformation (Figs 10c and 10d).

The behavior of microscrews with diameters between 1.3 and 1.6 mm was fairly similar (values of the variance in the stress of Dentaurum 1.5, Jeil 1.6, Mondeal 1.5, Spider Screw 1.5, MAS Microbite 1.3, and Tekka 1.5). For this range of diameters, Spider Screw 1.5 displayed the best variance behavior. The differences in the behavior of Jeil 2.0, Mondeal 2.0, and Tekka 2.0 with a shank diameter of 2.0 mm were substantially different, especially with Jeil 2.0, which was four times lower than Tekka 1.5.

Also apparent from Table 3, Jeil 1.6, Jeil 2.0, Mondeal 2.0, and Spider Screw 1.5 displayed less deformation. Similar values were obtained for Mondeal 1.5 and Tekka 1.5, which feature different designs and shapes (Tekka 1.5 is 1.35 mm in diameter and Mondeal 1.5 is 1.5 mm but with a 2.0-mm head).

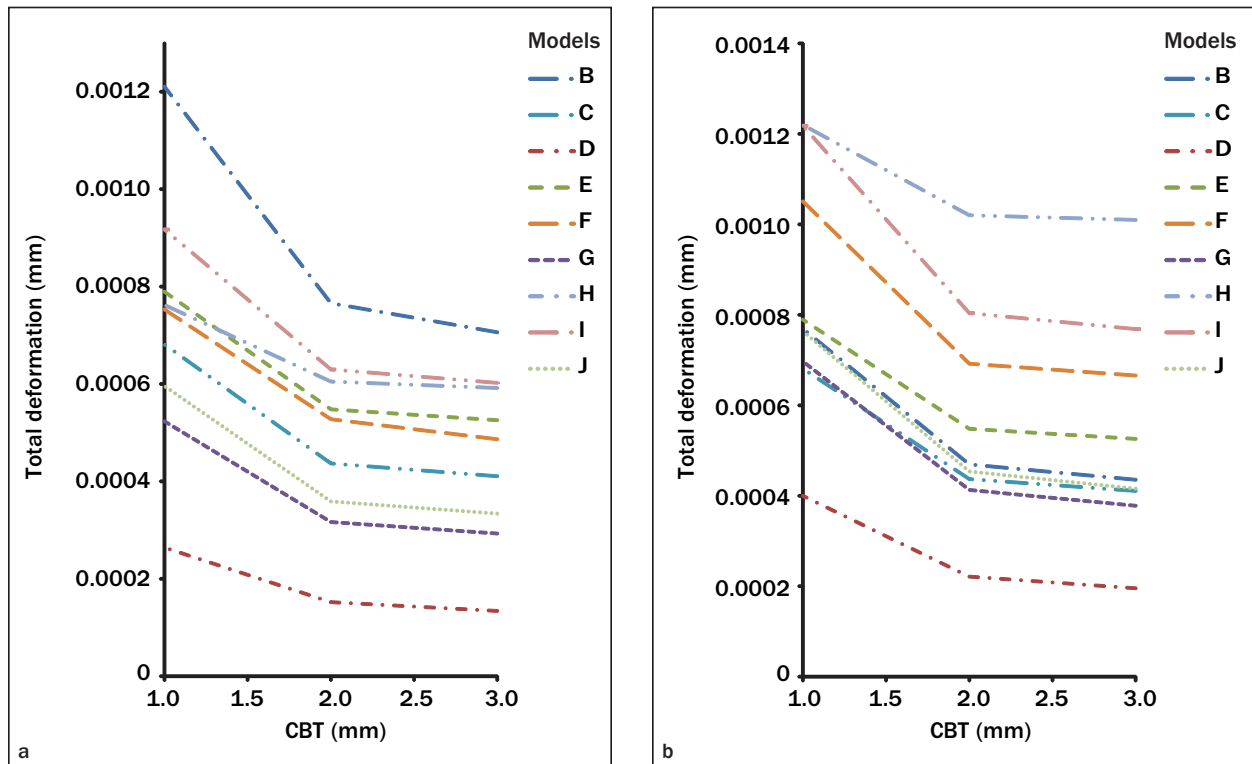


Fig 11 (a) Total deformation of the microscrews for DD of 8 mm at point C; (b) total deformation of the microscrews for DD of 6 mm at point C.

With respect to the length, head diameter, and shank length (Table 1) of each microscrew, and omitting the Abso Anchor 1.0, it is not possible to find a direct correlation between these geometric parameters and the behavior of each microscrew. Further work considering the thread shape, thread pitch, the shape of the shank, or other correlations between its geometric parameters should be done.

The most important finding about the variance behavior is that, for microscrews with the same design and shape (for example Tekka 1.5 and Tekka 2.0, Jeil 1.6 and Jeil 2.0), those with the wider diameter showed less variance in their values.

Behavior Near the Screw-Bone Junction (Point C)

When the microscrew is inside the bone, the fixation that the bone creates between itself and the microscrew (although some separation occurs when the frictionless contact is added) is very similar in each microscrew (point C of Fig 7) because it is outside the area where substantial differences are recorded in the deformations of the microscrew (points A and B).

Figures 11a and 11b show the deformation of each microscrew at point C (except for Abso Anchor 1.0, which has higher deformation values). Although

the difference between the highest deformation (Dentaurum 1.5) and the lowest (Jeil 2.0) was less than 10%, and taking into account the fact that this small deformation will increase in the head of the screw, it may be possible to consider the different behavior of each model in its root as an important factor to be included in clinical decision making.

It was in unfavorable situations (eg, thin cortical bone, shallow DD) where the differences between the behaviors of each microscrew were more substantial. Consequently, this is where each model can best be compared. At the shallower DD, Jeil 2.0 showed the lowest stress and least deformation, and Spider Screw 1.5 and, of course, Abso Anchor 1.0 (which, because of its higher values, was considered in the previous comparisons) displayed the highest stresses and greatest deformation.

The screws with a diameter of 2.0 mm (Jeil 2.0, Mondeal 2.0, Tekka 2.0) showed the best results when the DD is 8 mm. However, in the unfavorable situation of a 6-mm DD, their behavior changed: it improved for Dentaurum 1.5 and Jeil 1.6, and it worsened for Mondeal 1.5, Spider Screw 1.5, and Tekka 1.5. These differences may be explained by the different designs of each microscrew. On a microscopic level, for example, it can be seen that Dentaurum 1.5 has the widest threads.

CONCLUSIONS

With respect to the results obtained for each micro-screw, the following conclusions can be made:

1. It seemed that the final position of the microscrew did not have an important influence in the behavior of microscrews with larger diameters. In the case of narrower-diameter screws, the final position could affect the behavior of the microscrew (with differences of three- or fourfold).
2. At the same drilling depth, microscrews with a large head were more unstable, as evidenced by the values obtained for stress and deformation. The values can change dramatically.
3. In favorable situations, microscrews with a diameter of 1.5 mm showed similar behavior, and in unfavorable situations, microscrews with a conical shape showed the worst behavior, with higher stresses and deformations.
4. The study of the screw-bone joint in unfavorable situations showed how the microscrew design influences stability. It seems that the shape of the threads can explain differences in behavior (for example, the threads of Dentaurum 1.5 are larger than the threads of the other microscrews examined).
5. The optimal characteristics of a microscrew should be the following: diameter of 2 mm, cylindrical shape, short and wide head, short and wide shank, and appropriately sized threads. This is a microscrew with a large bone shape forming a compact and uniform design.
6. Of all the models analyzed in this work, Jeil 1.6 and Jeil 2.0 displayed the best behavior.

Summarizing the conclusions and considering only the results obtained in these computational simulations, it can be concluded that the shape and geometry of a microscrew are more important in its behavior and have strong influences on the maximum values of stress and deformation. The diameter of the microscrews is the most important geometric parameter.

ACKNOWLEDGMENTS

The authors gratefully acknowledge the many contributions by colleagues in the Escola Tècnica Superior d'Enginyeria Industrial i Aeronàutica de Terrassa (ETSEIAT), especially Professors Montserrat Pepió and Maria Victòria Cano, for their contribution to this work. The authors reported no conflicts of interest related to this study

REFERENCES

1. Motoyoshi M, Yoshida T, Ono A, Shimizu N. Effect of cortical bone thickness and implant placement torque on stability of orthodontic mini-implants. *Int J Oral Maxillofac Implants* 2007;22:779–784.
2. Holmgren EP, Seckinger RJ, Kilgren LM, Mante F. Evaluating parameters of osseointegrated dental implants using finite element analysis—A two-dimensional comparative study examining the effects of implant diameter, implant shape, and load direction. *J Oral Implantol* 1998;24:80–88.
3. Miyawaki S, Koyama I, Inoue M, Mishima K, Sugawara T, Yamamoto T. Factors associated with the stability of titanium screws placed in the posterior region for orthodontic anchorage. *Am J Orthod Dentofac Orthop* 2003;124:373–378.
4. Zienkiewicz OC, Zhu JZ. The superconvergent patch recovery and a posteriori error estimators. Part 1: The recovery technique. *Int J Numer Methods Eng* 1992;33:1331–1364.
5. Zienkiewicz OC, Zhu JZ. The superconvergent patch recovery and a posteriori error estimators. Part 2: Error estimates and adaptivity. *Int J Numer Methods Eng* 1992;33:1365–1382.
6. Doblaré M, García JM, Gómez MJ. Modelling bone tissue fracture and healing: A review. *Eng Fracture Mech* 2004;71:1809–1840.
7. Wilmes B, Rademacher C, Olthoff G, Drescher D. Parameters affecting primary stability of orthodontic mini-implants. *J Orofac Orthop* 2006;67:162–174.
8. Jiang L, Kong L, Li T, Gu Z, Hou R, Duan Y. Optimal selections of orthodontic mini-implant diameter and length by biomechanical consideration: A three-dimensional finite element analysis. *Adv Eng Softw* 2009;40:1124–1130.
9. Motoyoshi M, Ueno S, Okazaki K, Shimizu N. Bone stress for a mini-implant close to the roots of adjacent teeth—3D finite element analysis. *Int J Oral Maxillofac Surg* 2009;38:363–368.
10. Baggi L, Cappelloni I, Maceri F, Vairo G. Stress-based performance evaluation of osseointegrated dental implants by finite-element simulation. *Simul Model Pract Theory* 2008;16:971–987.
11. Kong L, Zhao Y, Hu K, et al. Selection of the implant thread pitch for optimal biomechanical properties: A three-dimensional finite element analysis. *Adv Eng Softw* 2009;40:474–478.
12. Ekici B. Numerical analysis of a dental implant system in three-dimension. *Adv Eng Softw* 2002;33:109–113.